JOC*Article*

Synthesis of Cage-Type Molecules with π-Cavity and Selective Gas-Phase Cation Complexation

Jeongryul Kim, Young Kook Kim, Nokyoung Park, Jong Hoon Hahn,* and Kyo Han Ahn*

Department of Chemistry and Center for Integrated Molecular Systems, Division of Molecular and Life Sciences, San 31 Hyoja-dong, Pohang 790-784, Republic of Korea

ahn@postech.ac.kr

Received April 4, 2005

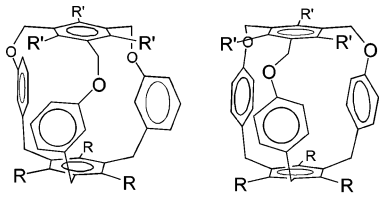

3 **4**

Cage-type molecules composed of phenyl walls and caps were synthesized as hosts for the binding of ammonium and alkali metal cations through cation$-\pi$ interactions. The synthesis involved a key cyclization step, which was markedly dependent on the capping component. Binding studies by electrospray ionization mass spectrometry toward lithium, sodium, potassium, and ammonium cations showed that the cage-type molecules selectively form a 1:1 complex. A competitive binding study showed that cage **3c** (R = Et, R′ = OMe) has a preference toward lithium cation while cage **4b** (R = Me, R′ = OMe) has a similar preference toward both lithium and ammonium ion in the presence of others. This selectivity pattern was tentatively explained by the gate size of the cage-type compounds, not by their cavity size.

Introduction

Cage-type molecules as molecular hosts have attracted considerable research interest from supramolecular chemists. Cage-type molecules are unique in that they can have finite and structurally well-defined cavities. Thus, molecular interactions between cage-type molecules and guests can provide size- and shape-dependent guest selectivity, in addition to an insight into the molecular recognition phenomena in a confined space. Cage-type molecules having arene interiors are of special interest because they can host alkali metal cations through so-called "cation$-\pi$ interactions". Since the first experimental report of the cation$-$arene interaction by Kebarle and co-workers,[1] both theoretical and experimental investigations on cation$-\pi$ interactions have elucidated their important role in a variety of molecular interactions.[2] We became interested in the cage-type host that is mainly composed of π-electron components, which, with its confined cavity, may provide an enriched π-donor environment toward cations such as alkali metal and ammonium ions. Although a variety of cage-type molecules are known,[3] most of them have large cavities or contain donor atoms that bind cations. Only a few examples of designed "π-receptors" are known for the cations. Vögtle and co-workers previously reported novel cation$-\pi$ receptor molecules, spheriphane **1** and its analogues. Although spheriphane **1** showed little extractability toward Na^+, one of its larger analogues showed high extractability toward Ag^+ ion.[4] Shinkai and co-workers reported "cavity size-selective" guest complexation using

(1) Sunner, J.; Nishizawa, K.; Kebarle, P. *J. Phys. Chem.* **1981**, *85*, 1814−1820.

(2) For a review on the cation$-\pi$ interactions, see: J. C. Ma, D. A. Dougherty, *Chem. Rev.* **1997**, *97*, 1303−1324.

(3) For some selected examples, see: (a) Colquhoun, H. M.; Arico, F.; Williams, D. J. *Chem. Commun.* **2001**, 2574−2575. (b) Kurata, H.; Nakaminami, H.; Matsumoto, K.; Kawase, T.; Oda, M. *Chem. Commun.* **2001**, 529−530. (c) Bucher, C.; Zimmerman, R. S.; Lynch, V.; Sessler, J. L. *J. Am. Chem. Soc.* **2001**, *123*, 9716−9717. (d) Takemura, H.; Nakshima, S.; Kon, N.; Yasutake, M.; Shinmyozu, T.; Inazu, T. *J. Am. Chem. Soc.* **2001**, *123*, 9293−9298. (e) Araki, K.; Hayashida, H. *Tetrahedron Lett.* **2000**, *41*, 1807−1810. (f) Kunze, A.; Bethke, S.; Gleiter, R.; Rominger, F. *Org. Lett.* **2000**, *2*, 609−612. (g) Mascal, M.; Kerdelhué, J.-L.; Blake, A. J.; Cooke, P. A. *Angew. Chem., Int. Ed.* **1999**, *38*, 1968−1971. (h) Vögtle, F.; Ibach, S.; Nieger, M.; Chartroux, C.; Krüger, T.; Stephan, H.; Gloe, K. *Chem. Commun.* **1997**, 1809−1810. (i) Davis, A. P.; Wareham, R. S. *Angew. Chem., Int. Ed. Engl.* **1998**, *16*, 2270−2273. (j) O'Krongly, D.; Denmeade, S. R.; Chiang, M. Y.; Breslow, R. *J. Am. Chem. Soc.* **1985**, *107*, 5544−5545. (k) Kang, H. C.; Hanson, A. W.; Eaton, B.; Boekelheide, V. *J. Am. Chem. Soc.* **1985**, *107*, 1979−1885.

(4) Gross, J.; Harder, G.; Vögtle, F.; Stephan, H.; Gloe, K. *Angew. Chem., Int. Ed. Engl.* **1995**, *34*, 481−484.

10.1021/jo050654w CCC: $30.25
Published on Web 08/05/2005

calix[4]arene and its derivatives by electrospray ionization mass spectrometry (ESI-MS).[5] Recently, Gokel and co-workers also reported size-selective π-complex formation using pyxophane **2** in the gas phase.[6] Herein, we wish to report the synthesis of novel cage-type molecules **3** and **4** that have π-cavity. These cage-type molecules are expected to have conformationally rigid and compact π-cavity. A comparative ESI-MS study toward alkali metal ions (Li^+, Na^+, and K^+) and NH_4^+ shows that these cage-type molecules selectively recognize Li^+ and NH_4^+, which may be explained by "gate-selective" complexation.

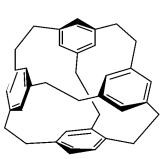

1

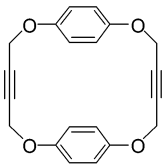

2

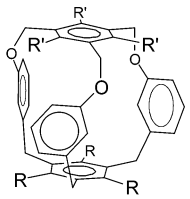

3

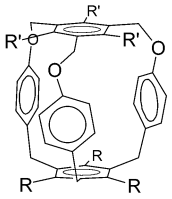

4

Results and Discussion

Synthesis and Structure Analysis of the Cage-Type Molecules. The compounds **3** and **4** consist of three phenyl rings as "walls" and two phenyl rings as top and bottom "caps". We have chosen 1,3,5-tris(bromomethyl)-2,4,6-(trimethyl)benzene and its triethyl analogue **5** as the capping components, which are known to have preorganized conformations readily. A molecular modeling study suggested that π-cage **3** has less ring strain than that of **4**, although the latter has a better cage shape. We first studied the synthesis of less strained **3**. The intermediate **7a**, which has both bottom and wall phenyl rings, was synthesized in a high yield by Cu(I)-catalyzed coupling of the Grignard reagent that was prepared from 3-(benzyloxy)bromobenzene (**6**) and tribromide **5a** (Scheme 1).[7] Similarly, **7b** was synthesized, in which case the yield was lower probably due to increased steric hindrance. Next, the phenol derivative **7a** was subjected to the coupling reaction with the capping component **5a** in the presence of Cs_2CO_3 in DMF at 80 °C; however, the desired compound **3a** was obtained in a very low yield (Scheme 1).

Changing the base and solvent resulted in no improvement. The coupling reaction between the 2,4,6-triethyl-based wall **7b** and the capping component **5b** did not give the corresponding cage product at all. After much experimentation, we finally overcame this problem by changing the capping component from **5a/5b** to the trimethoxy analogue **5c**. Treatment of **7a** with the new

SCHEME 1

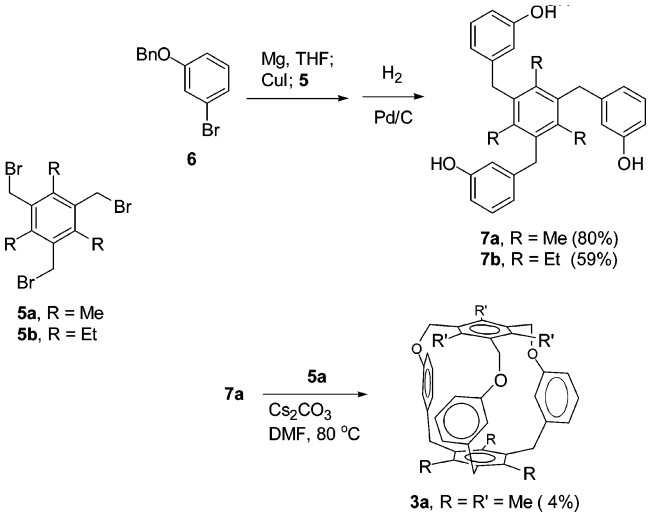

SCHEME 2

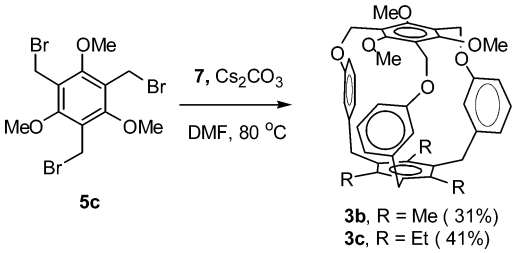

capping component **5c** under the same coupling conditions resulted in the corresponding cage-type molecule **3a** in 31% yield. This coupling yield increased to 41% in the case of **3c** (Scheme 2). *Thus, by changing the capping component, we were able to improve the coupling yield dramatically*.

A possible reason for the marked increase in the coupling yields by changing the capping component may be explained by neighboring group participation: The methoxy group in **5c** may assist the phenoxide attack at the nearby benzylic carbon mediated by the cesium cation. Similarly, we were able to synthesize cage-type molecule **4b**, a *para* analogue of **3**, by coupling the capping component **5c** with tris(phenol) **9** (Scheme 3). In this case, the yield decreased to 16%, which is probably due to the increased ring strain.

All of the cage-type molecules exhibited symmetric structures in solution, as judged from their simple NMR spectra. The symmetric structures were also evident from molecular modeling studies[8] that showed C_3-symmetric structures. The three phenyl walls are pointing outward in a screw-sense. Such a conformation was also identified in solution, judged from their ^1H NMR spectra: For example, in the cases of **3b** and **3c**, the isolated proton of the phenyl walls (6.18 ppm) appeared at an unusually upfield-shifted region from other protons (7.05−7.32 ppm), owing to a diamagnetic shielding from the bottom phenyl ring expected in such a conformation. The upper and bottom phenyl caps are slightly deviated from complete eclipsing when viewed from the top (Figure 1).

(5) Inokuchi, F.; Miyahara, Y.; Inazu, T.; Shinkai, S. *Angew. Chem., Int. Ed. Engl.* **1995**, *34*, 1364−1366.

(6) Behm, R.; Gloeckner, C.; Grayson, M. A.; Gross, M. L.; Gokel, G. W. *Chem. Commun.* **2000**, 2377−2378.

(7) Kim, Y. K.; Ha, J.; Cha, G.; Ahn, K. H. *Bull. Korean Chem. Soc.* **2002**, *23*, 1420−1424.

(8) The molecular modeling study was carried out at AM1 level using a program, PC Spartan Pro, purchased from Wave Function, Inc. (www.wavefun.com).

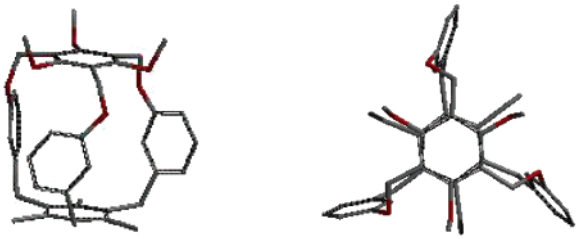

FIGURE 1. Calculated structure of *meta*-cage **3b**: side and top views.

SCHEME 3

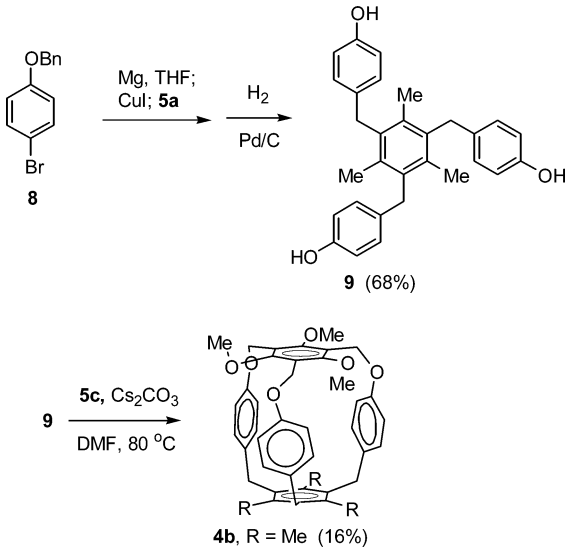

The cavity of *meta*-cage **3b** or **3c** can be viewed as a cylinder with a height of 6.2 Å (the distance between the phenyl base and cap) and a diameter of 5.9 Å.[9] If we account for the arene thickness (3.4 Å) and the tilt angle, the maximum cylindrical cavity size to accommodate guests could be estimated to be 2.8 Å (height) × 3.4 Å (diameter). This cavity may accommodate K^+ whose diameter is 2.7 Å. However, a space-filling model of the cage showed that not the cavity size but the gate size seemed to be a limiting factor toward guests in the static state described. The maximum gate size was estimated to be 2.1 Å in the case when the two phenyl walls were in a parallel position. However, such maximum opening would be an extreme case, and therefore, the gate does not seem to be large enough even for Na^+ to pass it readily, whose diameter is 1.98 Å.

The *para*-cage compound **4b** has a much better cylindrical shape compared with the *meta*-cage **3b**. The cavity of **4b** can also be viewed as a cylinder with a height of 6.6−6.7 Å and a diameter of 5.9 Å, as discussed above. The phenyl cap and base are completely eclipsed from each other when viewed from the top.[8] An appealing feature of this *para* analogue is that the three phenyl walls surround the caps, providing an ideal π-cavity. Such a favorable orientation of the phenyl walls was supported by ^{1}H NMR analysis: All of the protons of the phenyl walls appeared in the range of 6.37−6.43 ppm, and no unusually upfield-shifted peaks were observed in contrast

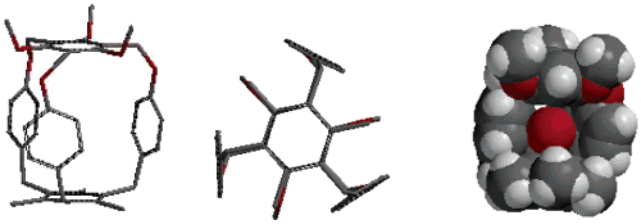

FIGURE 2. Calculated structures of *para*-cage **4b**. From left: side and top views and a K^+-nestled structure. (K^+: the red sphere in the center. One phenyl wall was removed for a better view.)

to the cases of *meta*-cages **3**. In the case of cage **4b**, the cavity size was estimated to be 3.2 Å (height) × 3.4 Å (diameter), which may accommodate K^+ (Figure 2).

Both the cage-type molecules **3** and **4** have ethereal oxygen atoms, which are introduced only for a synthetic reason. The ethereal oxygen atoms, however, do not seem to actively participate in the guest binding for two reasons: (1) they are phenolic oxygen atoms, which have minimal electron donacity, and (2) the oxygen lone pairs are directed outward before and after binding a guest in the cavity. In addition, the space-filling model showed that the ethereal oxygen atoms do not have contact with K^+.

Binding Studies. Even though *para*-cage **4b** seems to provide an ideal π-cavity toward cations, particularly K^+ and NH_4^+ ions, by the molecular modeling study, attempts to evaluate its binding ability toward these ions by NMR and extraction experiments were fruitless; hence, we concluded that cation−π interactions alone may not be enough for assessing their molecular interactions toward the cations by these experiments. Thus, a more sensitive method is required to evaluate the molecular interactions that involve mainly cation−π interactions. The evaluation of binding capability of the cage-type molecules **3c** and **4b** has been carried out by electrospray ionization−mass spectrometry. The ESI−MS is a very sensitive and powerful method for studying weak molecular interactions in the gas phase.[10] Three different experiments were carried out with *meta*- and *para*-cages **3c** and **4b**. First, for each cation (Li^+, Na^+, K^+, and NH_4^+), the ESI−MS experiment was conducted under the same conditions. Second, competition experiments were carried out using an equimolar mixture of all the cations. Third, for each of the cations and cages, the formation of "external" 2H/1G complexes[6] was checked separately. Each sample solution was prepared by dissolving 10 molar equiv of the cation (perchlorate salts) into a 1.3 mM solution of a cage in $CHCl_3$−MeOH (2:1, by volume). The ESI−MS analysis was carried out under fixed conditions: running solvent, $CHCl_3$; injection volume, 10 μL; flow rate, 10 μL/min; inlet temperature, 75 °C; scan rate, 300 data/s (1 scan/2.1 s, total 20 acquisitions); mass range, 400−1000 Da (300−1600 Da for the dimer detection experiments).

The complexation study between the host (cage **3c**, **4b**) and each cation guest by ESI−MS gave several interesting results. The mass peak of a 1:1 complex was observed for each of the cations examined (Li^+, Na^+, K^+, NH_4^+) in

(9) The diameter can be estimated as that of a sphere that contacts with all three phenyl walls.

(10) Cech, N. B.; Enke, C. G. *Mass Spectrom. Rev.* **2001**, *20*, 362−387.

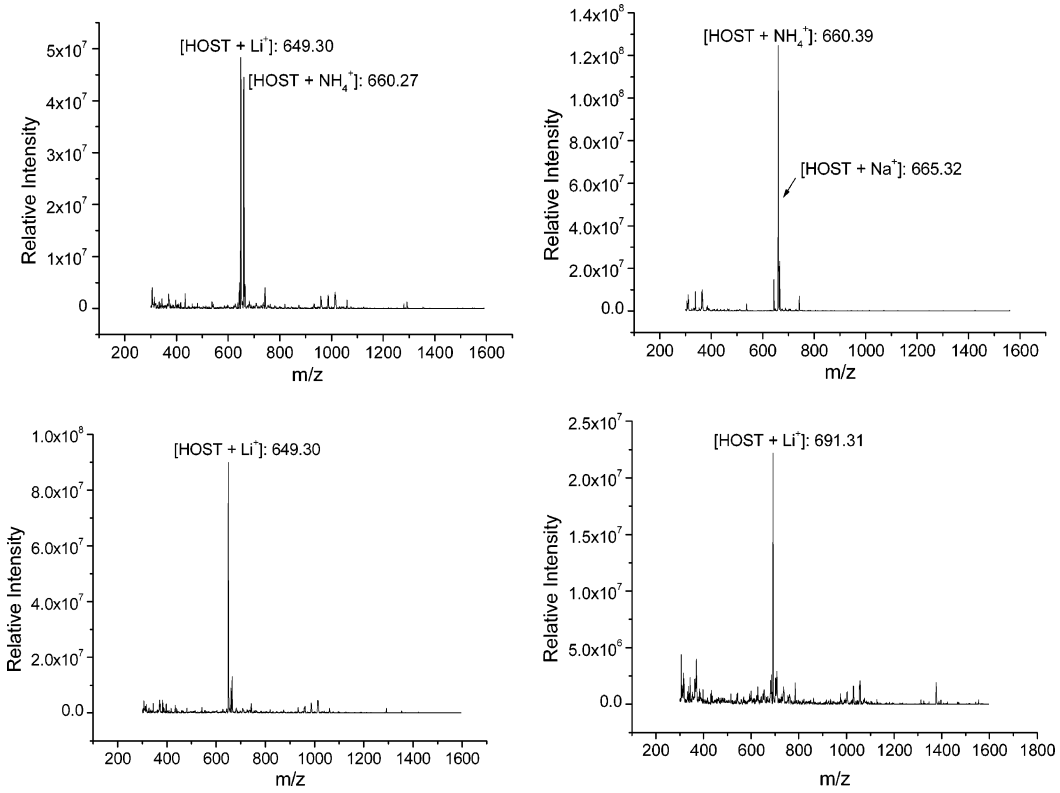

FIGURE 3. ESI spectra for (a) **4b** and a mixture of all the guests, (b) **4b** and the Li^+-omitted guest mixture, (c) **4b** and the NH_4^+-omitted guest mixture, and (d) **3c** and a mixture of all the guests.

the case of both cage compounds. For example, in the case of *para*-cage **4b**, a peak at $m/z = 649$ corresponding to a complex **4b**·Li^+ was observed along with traces of other peaks under the experimental conditions. Similarly, a peak at $m/z = 665$ corresponding to a **4b**·Na^+ complex was observed as the dominant peak. In the case of the NH_4^+ guest, a minor host peak was accompanied with a 1:1 adduct peak in a ratio of 1.0:5.7. In the case of the K^+ guest, a complex fragment pattern was observed with the corresponding **4b**·K^+ peak. In the case of *meta*-cage **3c**, similar but slightly different peak patterns were observed toward the guest cations: A slight difference in the relative intensity of 1:1 host−guest peak with respect to the host or other minor peaks were observed. For example, in the case of the NH_4^+ guest, the host and 1:1 complex peaks were observed with similar intensity.

The observation of a 1:1 host−guest peak for each of the cations examined suggests that the ESI−MS experimental conditions provide a dynamic process, in which larger cations such as Na^+ and K^+ overcome the energy barrier to pass the rather narrow gate of **3c** and **4b**, respectively. Thus, the separate ESI−MS experiment for each cation provided little information on the relative binding affinity or a possible gate-selective complexation process. However, the competition experiments provided valuable information on these aspects. When an equimolar mixture of Li^+, Na^+, K^+, and NH_4^+ was mixed with para-cage **4b** and subjected to ESI−MS analysis under conditions otherwise identical to those of the separate experiment, only two major adduct peaks of Li^+ and NH_4^+ were observed, with almost the same intensity. When either Li^+ or NH_4^+ was removed from the guest mixture, only the other major peak (NH_4^+- or Li^+-complex) was observed in each case (Figure 3, b and c). In the case of *meta*-cage **3c**, a different pattern resulted: In the presence of all of the cations, only its Li^+ complex was observed as the major peak and its NH_4^+ complex was not observed. When we removed Li^+ from the guest mixture, a complex peak pattern resulted which included four major peaks of the host, NH_4^+ and Na^+ complexes, and unknown. In both cases, we could observe a 2H/1G complex of Li^+ (at $m/z = 1376$) or NH_4^+ (at $m/z = 1388$, in the absence of the Li^+ guest) as a minor peak, with an intensity of ~5% of that of the major peak.

These ESI−MS data indicate that, in the presence of other cations, cage **4b** selectively binds both Li^+ and NH_4^+ with similar affinity, whereas **3c** binds Li^+ only. How can we interpret these ESI−MS data? The observed preference of both the host **3c** and **4b** toward Li^+ in the presence of other cations may be explained by evoking a gate-selective binding process. Otherwise, *para*-cage **4b** might have shown some selectivity toward K^+ in view of its complementary cavity size, according to our modeling study (Figure 2). Shinkai and co-workers reported size-dependent complexation of calixarene-based hosts under similar ESI−MS experimental conditions.[5] Also, Gokel's pyxophane **2** showed size selectivity toward Na^+.[6] Then, how can we explain the observed affinity of *para*-cage **4b** toward NH_4^+, which is similar to K^+ in size but different in shape? A possible explanation is that some ethereal oxygen atoms of the phenyl cap and walls may interact with NH_4^+ through hydrogen bonding. A modeling study, however, suggested that such hydrogen bonding is not likely because, in these cases, possible tripodal hydrogen bonding is geometrically not favorable. If such hydrogen-bonding interactions were operating, we would

have not observed the difference in the guest selectivity between *meta*-cage **3c** and *para*-cage **4b**. Thus, a different binding process may be proposed in this case. The NH_4^+ ion may slide into the cavity in a "dissociative" fashion: H^+ followed by NH_3 sliding through the gate. Once in the cavity, the NH_4^+ ion can have good contact with the surrounding aryl groups. In the case of *meta* analogue **3c**, such a sliding entry is also possible, but, because of its poor cavity-like shape, the inclusion complex would be less favored than the case of **4b**.[11]

Conclusion

We have synthesized cage-type molecules **3** and **4** as potential hosts for the selective recognition of alkali metal and ammonium cations mainly through cation−π interactions. The synthesis involved a key cyclization step, of which yield was markedly dependent on the capping component. The cage-type hosts have a π-cavity that is expected to accommodate a K^+ ion by a molecular modeling study. However, competitive binding studies by electrospray ionization mass spectrometry showed that **3c** binds selectively Li^+ while **4b** binds both Li^+ and NH_4^+ in the presence of other cations examined. A gate-selective binding process may explain these results. Under such a process, a dissociative binding process explains the complexation of host **4b** with NH_4^+. A structural modification of cage-type host **4b** to address the gate-selective binding process is under investigation.

Experimental Section

General Methods. ^{1}H NMR spectra are reported as follows: chemical shift in ppm from internal tetramethylsilane on the delta scale, multiplicity, coupling constant (in hertz), and integration. Melting points are uncorrected ones. Chromatography means flash column chromatography using silica gel of 230−400 mesh. Solvents were dried and distilled under standard conditions before use.

1-Bromo-3-benzyloxybenzene (6). To a stirred solution of sodium hydride (720 mg, 18 mmol, 60% dispersion in mineral oil) in DMF (20 mL) was added 3-bromophenol (2.6 g, 15 mmol) at a water−ice bath temperature under argon atmosphere, and the resulting mixture was stirred for 20 min at the same temperature. To the mixture was added benzyl bromide (1.8 mL, 15 mmol), the ice bath was removed, and the mixture was stirred at ambient temperature for 2 h. The reaction mixture was treated with a saturated aqueous ammonium chloride solution (5 mL) and diluted with diethyl ether (30 mL). The organic layer was dried and concentrated, and the residue was purified by chromatography (hexane/EtOAc, 9:1) to afford **6** as a white solid (4.0 g, 100% yield): $R_f = 0.6$ (hexane/EtOAc, 9:1); mp 61−62 °C; ^{1}H NMR ($CDCl_3$) δ 5.06 (s, 2H), 6.88−6.91 (m, 1H), 7.07−7.16 (m, 3H), 7.31−7.41 (m, 5H); ^{13}C NMR ($CDCl_3$) δ 160.2, 137.0, 131.2, 129.3, 128.8, 128.2, 124.7, 123.5, 118.8, 114.5, 70.8; MS (EI) *m/z* calcd for $C_{13}H_{11}BrO$ 262.00 $[M]^+$, found 262.05.

1-Bromo-4-benzyloxybenzene (8). This compound was similarly synthesized as above from 4-bromophenol (3.46 g, 20 mmol) and benzyl bromide (2.4 mL, 20 mmol) in 92% yield (4.86 g) as a colorless liquid: $R_f = 0.7$ (hexane/EtOAc, 9:1); ^{1}H NMR ($CDCl_3$) δ 5.00 (s, 2H), 6.83 (d, $J = 8.7$ Hz, 2H), 7.21−7.39 (m, 7H); ^{13}C NMR ($CDCl_3$) δ 158.5, 137.2, 132.9, 129.3, 128.8, 128.1, 117.3, 113.7, 70.8; MS (EI) *m/z* calcd for $C_{13}H_{11}BrO$ 262.00 $[M]^+$, found 262.03.

1,3,5-Tris(3-hydroxybenzyl)-2,4,6-trimethylbenzene (7a). To a stirred suspension of magnesium powder (183 mg, 7.5 mmol) in THF (5 mL) were added **6** (1.32 g, 5.0 mmol) and 1,2-dibromoethane (one drop) at 25 °C under argon, and the resulting mixture was stirred for an additional 1 h. This Grignard solution was transferred dropwise to a mixture of 1,3,5-tris(bromomethyl)mesitylene **5a** (399 mg, 1.0 mmol) and CuI (19 mg, 0.1 mmol) in THF (5 mL) at 60 °C, and the resulting mixture was further stirred for 12 h at the same temperature. The mixture was allowed to warm to 25 °C and quenched with a saturated aqueous $NaHCO_3$ solution (10 mL). The resulting solution was diluted with EtOAc (10 mL), and the organic layer was washed with brine, dried, and concentrated in vacuo. The residue was filtered through a short pad of silica gel (hexane/EtOAc, 9:1) to give the coupled compound. This crude compound was dissolved in ethanol (30 mL) and was subjected to hydrogenolysis in the presence of 10 wt % Pd/C (100 mg) under H_2 atmosphere (about 1 atm) at 25 °C for 2 h. The reaction mixture was filtered through Celite, and the filtrate was concentrated. Purification of the residue by chromatography (hexane/EtOAc, 7:3) afforded **7a** (336 mg, 77%) as a white solid: $R_f = 0.3$ (hexane/EtOAc, 7:3); mp 251−253 °C; ^{1}H NMR ($CDCl_3$/DMSO-d_6) δ 2.14 (s, 9H), 4.05 (s, 6H), 6.44 (s, 1H), 6.60 (dd, $J = 2.3$, 7.5 Hz, 6H), 7.06 (t, $J = 7.8$ Hz, 3H), 8.68 (s, 3H); ^{13}C NMR ($CDCl_3$/DMSO-d_6) δ 157.1, 141.5, 134.4, 134.3, 129.1, 119.0, 114.3, 112.6, 35.7, 16.5; MS (FAB) *m/z* calcd for $C_{30}H_{30}O_3$ 439.22 $[M + 1]^+$, found 439.22.

1,3,5-Tris(3-hydroxybenzyl)-2,4,6-triethylbenzene (7b). This compound was similarly synthesized as above from **6** (1.32 g, 5.0 mmol) and 1,3,5-tris(bromomethyl)-2,4,6-triethylbenzene **5b** (441 mg, 1.0 mmol) in 59% yield (287 mg) as a white solid. $R_f = 0.3$ (hexane:EtOAc, 7:3); mp 200−201 °C; ^{1}H NMR ($CDCl_3$/DMSO-d_6) δ 1.11 (t, $J = 7.5$ Hz, 9H), 2.47 (q, $J = 7.5$ Hz, 6H), 4.01 (s, 6H), 6.35 (s, 3H), 6.62 (dd, $J = 1.8$, 7.9 Hz, 3H), 6.76 (d, $J = 7.5$ Hz, 3H), 7.12 (t, $J = 7.8$ Hz, 3H), 8.37 (s, 3H); ^{13}C NMR ($CDCl_3$/DMSO-d_6) δ 157.6, 143.2, 141.8, 134.3, 129.8, 120.2, 114.9, 113.4, 40.4, 34.8, 24.1, 15.6; MS (FAB) *m/z* calcd for $C_{33}H_{36}O_3$ 481.27 $[M + 1]^+$, found 481.28.

1,3,5-Tris(4-hydroxybenzyl)-2,4,6-trimethylbenzene (9). This compound was similarly synthesized as above from the bromobenzene derivative **8** (3.5 g, 13.3 mmol) and **5a** (1.06 g, 2.66 mmol) in 68% yield (791 mg) as a white solid: $R_f = 0.2$ (hexane/EtOAc, 7:3); mp 251−253 °C; ^{1}H NMR ($CDCl_3$/DMSO-d_6) δ 2.12 (s, 9H), 4.01 (s, 6H), 6.72 (d, $J = 8.3$ Hz, 6H), 6.83 (d, $J = 8.3$ Hz, 6H), 8.16(s 3H); ^{13}C NMR ($CDCl_3$/DMSO-d_6) δ 155.2, 135.7, 134.8, 131.7, 129.2, 115.9, 35.7, 17.1; MS (FAB) *m/z* calcd for $C_{30}H_{30}O_3$ 439.22 $[M + 1]^+$, found 439.23.

***meta*-Cage 3a.** To a stirred solution of Cs_2CO_3 (1.3 g, 4 mmol) in DMF (25 mL) at 80 °C under argon was added dropwise the phenolic compound **7a** (88 mg, 0.2 mmol) and **5a** (80 mg, 0.2 mmol) in DMF (15 mL) by a syringe pump for 6 h, and the resulting mixture was further stirred for 60 h at the same temperature. The mixture was cooled to room temperature, and the solvent was removed at low pressure. The residue was diluted with EtOAc (5 mL) and poured into brine (10 mL). The organic phase was dried, filtered, and concentrated in vacuo. Purification of the residue by chromatography (hexane/EtOAc, 4:1) afforded **3a (**25 mg**,** 4%) as a white solid: $R_f = 0.7$ (hexane/EtOAc, 7:3); mp 320−344 °C dec; ^{1}H NMR ($CDCl_3$) δ 2.06 (s, 9H), 2.21 (s, 9H), 3.95 (s, 6H), 5.11 (s, 6H), 5.89 (s, 3H), 7.05−7.09 (m, 6H), 7.28 (t, $J = 7.9$ Hz, 3H); ^{13}C NMR ($CDCl_3$) δ 160.1, 141.9, 137.7, 135.7, 134.0, 132.6, 129.5, 124.6, 120.7, 118.6, 70.8, 36.4, 17.5, 16.2; MS (FAB) *m/z* calcd for $C_{42}H_{42}O_3$ 595.31 $[M + 1]^+$, found 595.42.

***meta*-Cage 3b.** This compound was synthesized similarly as above by coupling of the *meta*-phenol derivative **7a** (46 mg, 0.104 mmol) with 1,3,5-tris(bromomethyl)-2,4,6-(trimethoxy)-benzene **5c** (47 mg, 0.104 mmol) in 31% yield (21 mg) as a

(11) Such a dissociative process, occurring under the dynamic process, may not achieve an equilibrium state; otherwise, the NH_4^+−inclusion complex with better size complementarity would be preferred over the Li^+ complex (From the results of Shinkai and co-workers,[4] it is expected that the NH_4^+−inclusion complex surrounded by four phenyl rings in an ideal case would be thermodynamically more favored over the Li^+ complex stabilized by one phenyl ring).

white solid: R_f = 0.5 (hexane/EtOAc, 4:1); mp 289−291 °C; ^{1}H NMR ($CDCl_3$) δ 2.19 (s, 9H), 3.15 (s, 9H), 3.96 (s, 6H), 5.00 (s, 6H), 6.18 (s, 3H), 7.05−7.12 (m, 6H), 7.32 (t, J = 7.8 Hz, 3H); ^{13}C NMR ($CDCl_3$) δ 161.3, 160.9, 142.0, 136.1, 134.6, 130.5, 125.5, 122.7, 121.6, 120.4, 68.4, 64.7, 36.7, 18.0; MS (FAB) *m/z* calcd for $C_{42}H_{42}O_6$ 643.30 $[M + 1]^+$, found 643.34.

***meta*-Cage 3c.** This compound was synthesized similarly as above by coupling of the *meta*-phenol derivative **7b** (96.1 mg, 0.2 mmol) with **5c** (89 mg, 0.2 mmol) in 41% yield (56 mg) as a white solid: R_f = 0.6 (hexane/EtOAc, 4:1); mp 309−311 °C dec; ^{1}H NMR ($CDCl_3$) δ 1.22 (t, J = 7.5 Hz, 9H), 2.51 (q, J = 7.5 Hz, 6H), 3.13 (s, 9H), 3.94 (s, 6H), 5.00 (s, 6H), 6.18 (s, 3H), 7.05−7.11 (m, 6H), 7.32 (t, J = 7.8 Hz, 3H); ^{13}C NMR ($CDCl_3$) δ 161.2, 160.9, 142.6, 141.1, 135.2, 130.5, 125.3, 122.6, 121.5, 68.3, 64.7, 35.2, 24.2, 15.5; MS (FAB) *m/z* calcd for $C_{45}H_{48}O_6$ 685.35 $[M + 1]^+$, found 685.33.

***para*-Cage 4b.** This compound was synthesized similarly as above by coupling of the *para*-phenol derivative **9** (132 mg, 0.3 mmol) with **5c** (134 mg, 0.3 mmol) in 16% yield (31 mg) as a white solid: R_f = 0.2 (hexane/EtOAc, 4:1); mp >310 °C dec; ^{1}H NMR ($CDCl_3$) δ 2.25 (s, 9H), 3.76 (s, 9H), 3.90 (s, 6H), 5.23 (s, 6H), 6.37 (d, J = 8.9 Hz, 6H), 6.43 (d, J = 8.9 Hz, 6H); ^{13}C NMR ($CDCl_3$) δ 160.0, 155.7, 140.7, 133.1, 131.9, 130.1, 121.3, 114.6, 63.2, 61.0, 35.1, 18.3; MS (ES) *m/z* calcd for $C_{42}H_{42}O_6$ 642.30 $[M]^+$, found 642.55.

Acknowledgment. We thank the Center for Integrated Molecular Systems/KOSEF for financial support of this work.

Supporting Information Available: ^{1}H and ^{13}C NMR spectra of compounds **7a**,**b**, **9**, **3a**−**c**, and **4b**; ESI MS data not shown in Figure 3. This material is available free of charge via the Internet at http://pubs.acs.org.

JO050654W